MADRID
inter.noise 2019
June 16 - 19
NOISE CONTROL FOR A BETTER ENVIRONMENT

Numerical prediction of interior noise due to fluctuation surface pressure with an idealized side mirror

Shao, Jianwang[1]
School of Automotive Studies, Tongji University
No 4800, RD Caoan, 201804, Shanghai, China

Zeng, Tao[2]
School of Automotive Studies, Tongji University
No 4800, RD Caoan, 201804, Shanghai, China

Wu, Xian[3,*]
School of Automotive Studies, Tongji University
No 4800, RD Caoan, 201804, Shanghai, China
*** Corresponding author**

Wang, Cheng[4]
School of Automotive Studies, Tongji University
No 4800, RD Caoan, 201804, Shanghai, China

ABSTRACT

The prediction of radiated sound of vibrated structures excited by aerodynamic load is determined by the convective component and acoustic component of the fluctuation surface pressure (FSP). And the method that is adopted to predict cabin interior noise depends on computing time, accuracy, design phase of a car, etc. In this paper, numerical prediction for sound radiated by a panel under low Mach flow past a side mirror is investigated in order to find out which method is the most appropriate to the cabin interior noise problem under aerodynamic load. The methods of Corcos model and modal force are used to obtain the convective component and the acoustic component is extracted from boundary element method (BEM). Then, the sound pressure levels (SPLs) radiated by the panel are gained of different methods which are Corcos model coupled with BEM, deterministic modal force method coupled with BEM and random modal force method coupled with BEM. Meanwhile, the wavenumber-frequency spectrum of separated area and reattached area are also compared. Through comparing with experimental data published in literature, it is found that the two methods of random modal force and Corcos model coupled with BEM can predict cabin interior noise better than the method of deterministic modal force coupled with BEM. Moreover, the method of

[1] shaojianwang@tongji.edu.cn
[2] zrtao220@163.com
[3] wuxian@tongji.edu.cn
[4] 1434338@tongji.edu.cn

Corcos model costs less computing time than the random modal force method for gaining the convective component of FSP. But, the results of random modal force coupled with BEM have better consistency with experimental data. These methods can provide some advices to how to quickly and accurately calculate vehicle interior SPL excited by aerodynamic load in the early stage of vehicle designing process.

Keywords: Noise, Fluctuation Surface Pressure, Mirror
I-INCE Classification of Subject Number: 76

1. INTRODUCTION

The wind noise sources generated by turbulent flow play an important role to the interior SPL of the vehicle. Both convective and acoustic components can be equally important contributors to noise transmission to the vehicle cabin although the turbulent boundary layer (TBL) pressure is 25 to 35 dB higher in level than the corresponding acoustic components[1]. Because the acoustic component has larger wavelengths that can be easily coupled with the radiating modes of the plate that includes mainly large wavelengths[2]. M. Smith, et al.[3] designed an experiment to analyze sound radiation of a car window under flow induced excitation, but no acoustic component was found due to aliasing effect. Later, Bremner[4] and F. G. Mendonca[5] demonstrated the existence of acoustic source through computational fluid dynamics (CFD) compressible flow simulation with wavenumber-frequency (k-ω) method. In order to capture the acoustic component, CFD compressible turbulent flow data are necessary if acoustic wind tunnel (AWT) is not available. Besides, there are many practical difficulties to separate out the acoustic components in AWT, such as, transducer size and locations, the background noise etc. Moreover, CFD compressible method is time-consuming and element size needs to be very small to capture acoustic component. However, CFD incompressible flow simulation costs less time and can be conducted easily. So, how to predict interior noise of the vehicle accurately based on CFD incompressible flow data is the concerned problem. Blanchet, D.[6] proposed several models to predict cabin interior noise based on CFD compressible, incompressible simulation or experiment results, but no comparison between different models was acquired. Therefore, in this paper, wavenumber-frequency spectrums of separated and reattached area are also analyzed. Three approaches are then proposed to predict radiated SPL of a panel under aerodynamic load. Accuracy of the results and computing time of these three different approaches are also compared to give some advices for predicting cabin interior noise.

2. ANALYSIS PROCEDURE

2.1 Calculation scheme

The main steps in the process are shown schematically in Figure 1. Firstly, CFD model is built to get FSP of side glass. Then several methods are taken to predict the radiated SPL of the panel excited by TBL. Corcos model, random modal force method and determine model force method are taken to represent convective component. Acoustic component is achieved by BEM method. Finally, both convective component and acoustic component are added on vibro-acoustic model of side glass to predict radiated SPL.

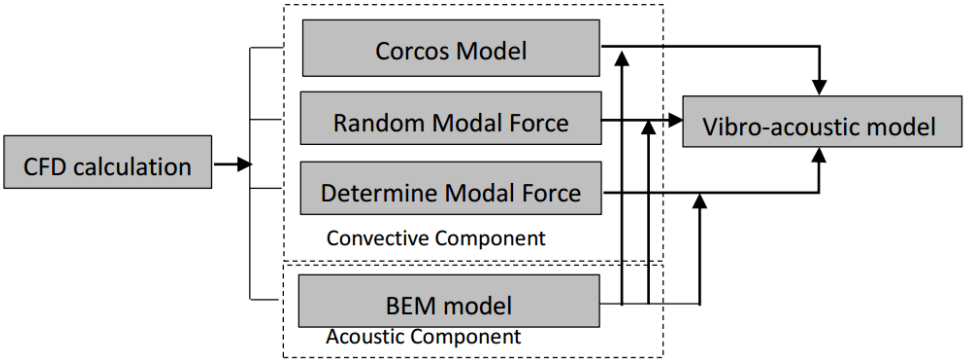

Fig. 1 – Process for predicting radiated SPL

The first model is that a BEM model propagating the acoustic waves from the FSP towards the side glass is built to evaluate the acoustic component. As for the convective component, it is extracted from the flow data to fit Corcos parameters. Therefore, a statistical energy analysis (SEA) panel is established to simulate the side glass and acoustic component is defined as Diffuse Acoustic Field (DAF) loaded on this SEA panel. The other two are that the time domain FSP is converted into deterministic or random modal forces and applied on a finite element panel. As for the deterministic modal force, the full time domain modal force signal is taken as a single window and applied as deterministic excitation on the vibro-acoustic model. The full time domain model force signal is also post-processed and averaged using overlapping segments to define the random modal force. The acoustic component is also gained by BEM method and defined as determine FSP projected on nodes of the finite element panel. In the following analysis, the parameters of the studied panel are shown in Table 1.

Table 1 – Panel parameters

Plate length a(m)	*0.8*
Plate width b(m)	*0.4*
Plate thickness h(m)	*0.004*
Structure damping factor c	*0.01*
Density of the plate ρ(kg/m^3)	*2700*
Young's Modulus E(N/m^2)	7×10^{10}
Poisson's Ratio ν	*0.33*

A rectangular plate is meshed using shell elements of size $\Delta_x = \Delta_y = 0.005m$, which is the same size as the separated area. The material of panel is aluminum and the measured point is illustrated in Figure 2(b), whose distance to the panel is 0.1m.

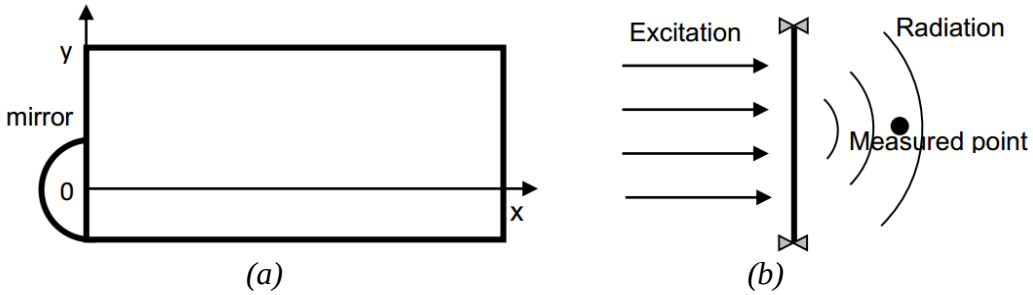

(a) *(b)*

Fig. 2 – Computational set-up. (a) size of studied panel in plane view; (b) radiated acoustic pressure field in side elevation

2.2 CFD Simulation

An idealized side mirror is selected as the study object, which is comprised by a half-cylinder and a quarter of a sphere. Parameters of the half cylinder and 1/4 sphere are shown in Figure 3(a). The side mirror is mounted on a flat plate. The length, width and height of the computational domain are illustrated in Figure 3(b). A structured hexahedral mesh is created in the entire domain in the commercial software ICEM. The mesh includes approximately seven million CFD cells and the quality of the mesh is very good. Near-wall layer extrusions is built to resolve the boundary and adverse-pressure-gradient flow separation with fine mesh. The CFD computing process is completed by software Fluent. The boundary conditions for the different surfaces bounding the computational domain are listed in Table 2.

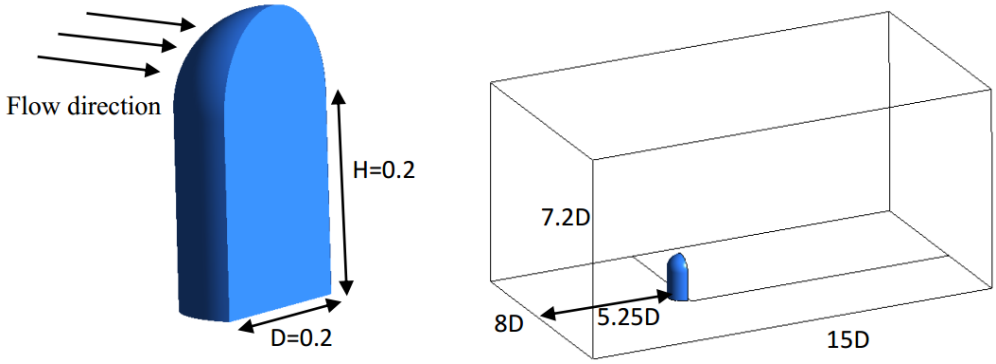

(a) *(b)*

Fig. 3 – Pre-process for CFD simulation. (a) Size of idealized side mirror; (b) Computational domain for flow

Table 2 – Boundary conditions

Boundary	*Boundary Condition*	*Value*
Inlet	*Constant Velocity*	*40m/s*
Outlet	*Constant pressure*	*0Pa(gage)*
Mirror	*No slip wall*	-
Ground	*No slip wall*	-
Other wall	*Symmetry*	-

Firstly, a steady CFD analysis is performed for flow past the idealized side mirror with realizable two equations k – ε(kinetic energy-dissipation rate) turbulent model. The steady time step is set to 1000. Then the steady state data is taken as initial condition of the transient CFD analysis. Siegert et al.[错误!未找到引用源。] and Y.P. Wang [错误!未找到引用源。] have demonstrated the high accuracy of Large Eddy Simulation (LES) to compute surface pressure and suitable to resolve small scale oscillations. So, LES is used to compute unsteady flow field of the side mirror and Smagorinsky-Lilly model is selected as sub-grid-scale (SGS) model. The transient simulation is started with a time segment of length 0.1 second using a time step size of 2e-5 second. After dynamic stability is achieved, another 0.12 second computing time is applied to sampling with the same time step size. Twenty solver iterations are conducted within each time step to ensure that the continuity and momentum equations are converged.

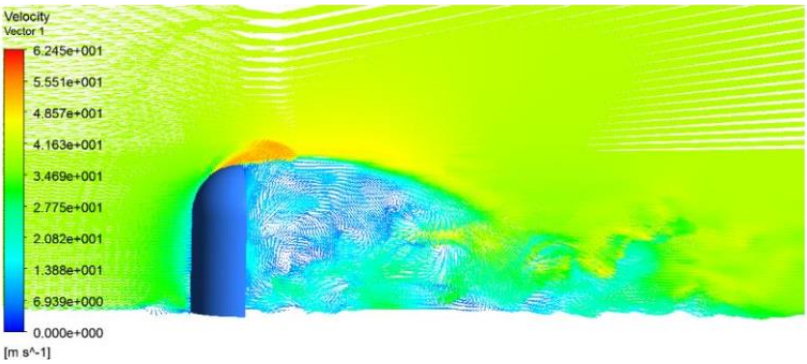

Fig. 4 – Velocity vectors of the side mirror

Figure 4 shows the velocity vectors of side mirror due to a free-stream velocity of 40m/s. The flow experiences strongly three-dimensional separation in the near-wake of the mirror, and then reattaches at approximately two mirror-heights downstream of the back face of the mirror.

The FSP is recovered for a rectangular region of dimension $1.7\text{m} \times 0.4\text{m}$ downstream of the side mirror. Three main regions can be observed, which are the mirror wake, a reattached region and a region without vortex (A-pillar was not considered in this case). These regions typically exhibit very different flow characteristics and can be modelled using several Corcos sources with parameters corresponding to each flow region. In this case, a single set of Corcos parameters would be adopted to represent the TBL of mirror separated region whose size is $0.8\text{m}\times0.4\text{m}$ and another set of Corcos parameters would be used to the reattached region with a size of $0.9\text{m}\times0.4\text{m}$. The discrepancy between these two regions would be compared.

2.3 Wavenumber-Frequency Analysis of Separated Area and Reattached Area

Wavenumber-frequency analysis is used to identify pressure power spectrum density (PSD) of separated area and reattached area, respectively, as illustrated in Figure 5. Positive wavenumber stands for acoustic propagation downstream in relation to fluid flow and negative wavenumber represents acoustic propagation upstream. No acoustic component is found because of CFD incompressible simulation. But both positive and negative wavenumber can be found in separated area, which agrees with the characteristics of vortex behind the mirror. And convective speed $U_c = 0.55U$(U is the flow velocity). However, only positive wavenumber can be seen in reattached area, which means the flow becomes uniform. And the convective speed $U_c = 0.7U$ is bigger than that in the separated area.

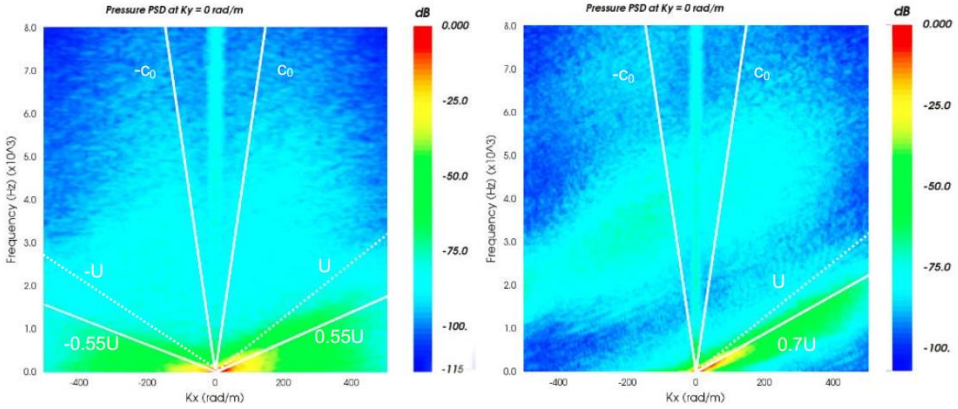

(a) *(b)*

Fig. 5 – Wavenumber-frequency spectrum analysis. (a) separated area; (b) reattached area

2.4 Methodology to Predict Radiated Sound

2.4.1 Results of convective component

The phase of the cross spectrum and the coherence between two any points can be used to evaluate Corcos parameters. After post-processing, four Corcos parameters (a convection velocity U_c, a decay coefficient spectra in the flow direction α_x, a decay coefficient spectra in the cross flow direction α_y and a pressure spectra $\Phi(\omega)$) are achieved in VA One [错误!未找到引用源。]. The space-average root mean square (RMS) pressure spectra is illustrated in Figure 6. It is the exterior surface pressure spectrum loading on the glass, where spectrum decreases quickly with frequency below 2000Hz. Most of the energy is concentrated at low frequency.

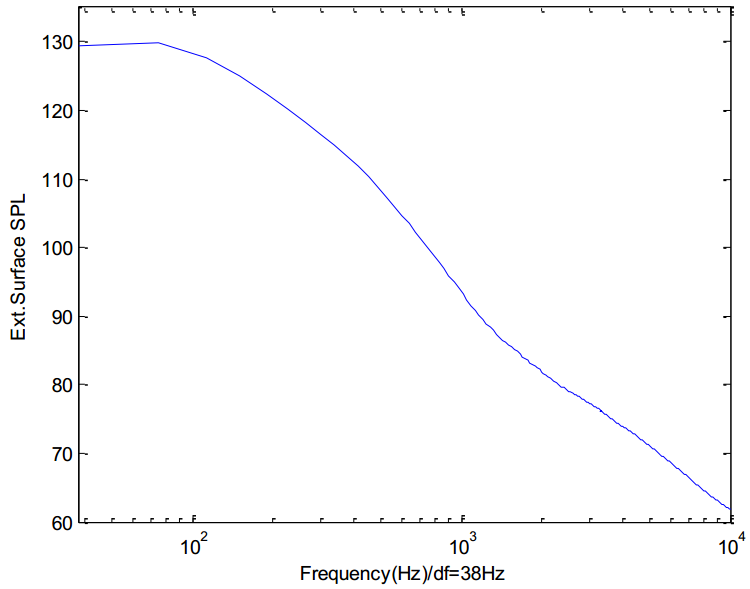

Fig. 6 – Space-average SPL obtained by Corcos model

It is necessary to obtain data for the surface pressure time histories for all nodes of the finite element panel for determine modal force and random modal force. The time-domain surface pressures are then convert into frequency-domain and no overlap is used to define as determine modal force. For random modal force, the pressure data is processed as a series of random signals using Welch's method where the time data is split into 8 segments with 50% overlapping. Fast Fourier transform (FFT) is applied to each segment and the pressure auto-spectra and cross-spectra are obtained as the average over all segments. The window option is set to Hamming.

2.4.2 BEM results

CFD time domain FSP coupled to a BEM and the Curle's integral version of the Lighthill equation is used to calculate surface source terms. It is then applied to the BEM fluid standing for external excitation of the side glass. The model is established in VA One and the panel is taken as data recovery surface. Space-average RMS surface pressure across the mirror face is gained while signal processing window is set to Hann, and subtract mean value is used to avoid pollution of the spectral content. Figure 7 shows that the space-average pressure of mirror Curle's source radiation onto the side glass panel. At middle-low frequency, FSP of the mirror decreases quickly. Most of the energy of FSP of the mirror lies at lower frequency.

The space-average pressure of the panel variation with frequency is gained based on the FM-BEM model. The pressure can then be defined either as FSP excitation on nodes of the panel or as DAF load on the SEA panel. The pressure magnitude RMS of the panel are shown in Figure 8. One can see that the acoustic energy concentrates near the mirror. Random loading on the mirror result in spatially random directivity of acoustic radiation on side glass panel. Besides, the acoustic energy becomes higher with frequency as shown in Figure 8 (a)-(d).

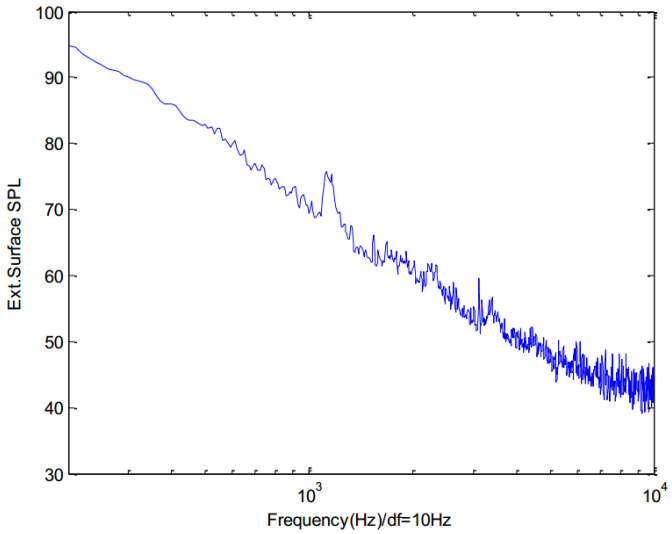

Fig. 7 – Space-average SPL of the mirror Curle's source radiation onto the side glass panel

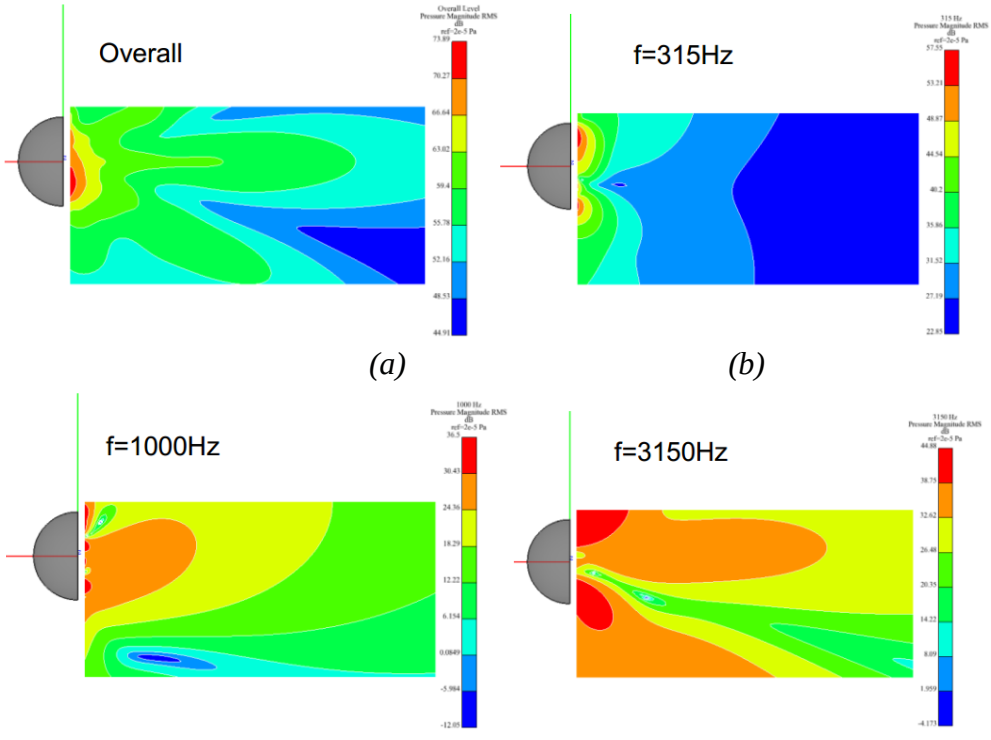

Fig. 8 – Results of CFD FSP of mirror applied as a boundary source term on a BEM model. (a) Overall level pressure magnitude RMS; (b) Pressure magnitude RMS at 315Hz; (c) Pressure magnitude RMS at 1000Hz; (d) Pressure magnitude RMS at 3150Hz

3. RESULTS ANALYSIS

3.1 Results of Corcos model Coupled with BEM

The Semi Infinite Fluid (SIF) (namely, the measured point in Fig. 2(b)) is arranged 0.1m away from the panel and at the center of the panel in order to validate the accuracy of different methods with experiment data conducted by Smith M.[3] in which the distance from the measured point to the panel is also 0.1m. Two excitations which are convective component results from Corcos model and acoustic component with DAF gained by FM-BEM are loaded on the panel. Then the radiated SPL of Corcos model with DAF and without DAF are computed, respectively, as illustrated in Figure 9.

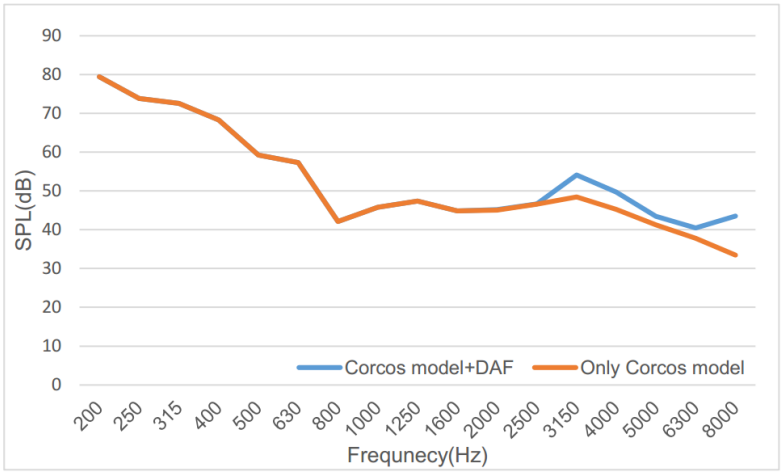

Fig. 9 – Radiated SPL of measured point with Corcos model coupled with BEM method. (Corcos model+DAF:convective component and acoustic component ; Only Corcos model:only convective component)

We can clearly see that the SPL of Corcos model with DAF over 2500Hz is much higher than that without DAF, which is consistent with the fact that the acoustic component dominates at high frequency, and the radiation SPL is almost the same under 2500Hz. The acoustic wavenumber k_a, the convective wavenumber k_c and the plate free wavenumber k_p are shown in Figure 10. The plate free wavenumber equals to the acoustic wavenumber at 3150Hz. So, radiated SPL reaches a peak at this frequency as illustrated in Figure 9. Another peak should appear at 23Hz, which is hydrodynamic coincidence.

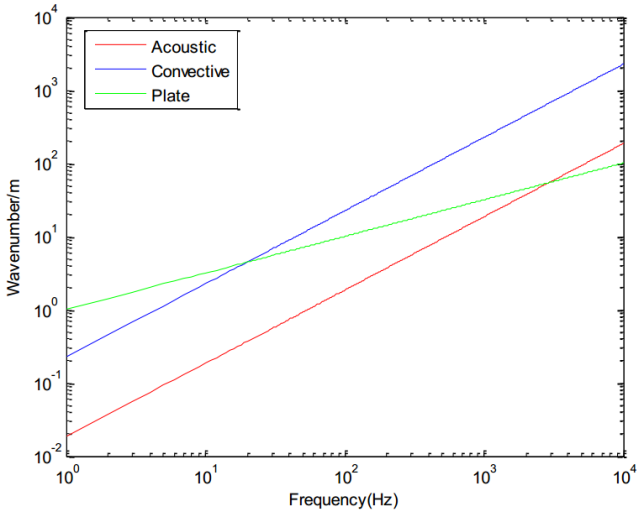

Fig. 10- Wavenumbers of convective, acoustic and plate. (Acoustic: Acoustic wavenumber; Convective: Convective wavenumber; Plate: Plate wavenumber)

3.2 Results of Random Modal Force Method Coupled with BEM

When the panel is finite element structure, the modal of this panel should be compute firstly. Because the test panel was fixed during the experiment, which was conducted by Smith M.[3], the panel in simulation is also set with the clamped boundary condition. Then both convective component and acoustic component can be projected onto the finite element (FE) panel nodes to compute the radiation acoustic field. The results of convective FSP with and without acoustic FSP are gained separately as shown in Figure 11. The radiated SPL of convective component with acoustic FSP is higher from 2500Hz, which is similar to the result found by Corcos model coupled with BEM method. But radiated SPL calculated by random modal force coupled with BEM method changes more greatly and two typical peaks can be found at 400Hz and at 4000Hz.

For a TBL excitation, the modal excitation term reaches maximum value when the convective wavenumber ($k_c = \omega/U_c$) is equal to the streamwise modal wavenumber of the panel ($k_m = m\pi/a$). So, the hydrodynamic coincidence may occur at any frequency. High excitation and resonance make contribution together to the radiated SPL. Therefore, the highest radiated SPL happens when the maximum value of modal excitation term occurs at the resonance frequency of the panel structure mode. The 5th and the 84th mode of the panel occurs at 398.49Hz and 4006.7Hz, respectively. So, two obvious peaks happen at 400Hz and 4000Hz.

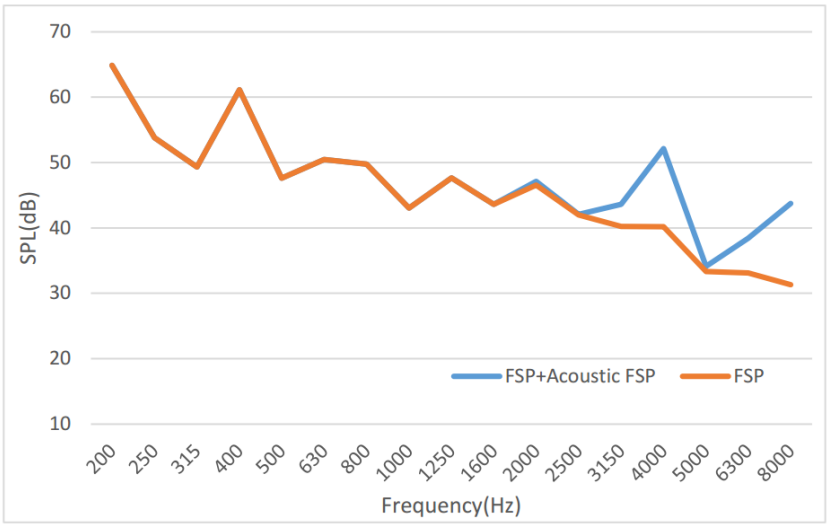

Fig. 11 – Radiated SPL of measured point with random modal force coupled with BEM. (FSP+Acoustic FSP:convective FSP and acoustic FSP; FSP:only convective FSP)

3.3 Results of Deterministic Modal Force Method Coupled with BEM

The computing process is almost the same with random modal force and the only one difference is that the convective component in time domain is used in its entirety as a single window and defined in the aero-vibration-acoustic model as a deterministic excitation. The result is gained as shown in Figure 12. Different from random modal force coupled with BEM method, the discrepancy of radiated SPL of convective FSP with and without acoustic FSP is pronounced at 1600Hz which may be due to aliasing effects. The two peaks become more evident and occur at the same frequency as deterministic modal force coupled with BEM method.

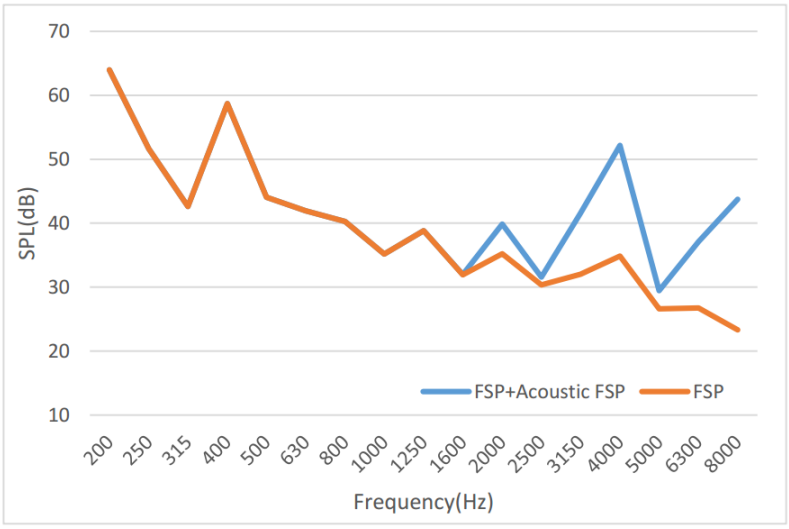

Fig. 12 – Radiated SPL of measured point with deterministic modal force coupled with BEM. (FSP+Acoustic FSP:convective FSP and acoustic FSP ; FSP:only convective FSP)

3.4 Comparison

The results which are achieved by above three different methods are drawn together with the test result which was gained by Bremner P.G.[4] . Figure 13 shows that radiated SPL based on random modal force coupled with BEM is higher than deterministic modal force coupled with BEM from 200-8000Hz. But the tendency of deterministic modal force coupled with BEM and random modal force coupled with BEM are almost the same especially at coincidence frequency. Radiated SPL of Corcos model coupled with BEM is close to that of random modal force coupled with BEM over 800Hz. But, there are some differences between Corcos model coupled with BEM and random modal force coupled with BEM below 630Hz. Because SEA method suffers from increasing variance at low frequency and modal overlap of the panel is much less than 1 below 500Hz. Through comparing with experimental data, random modal force coupled with BEM is recommended to predict radiated SPL under aerodynamic load at middle-low frequency.

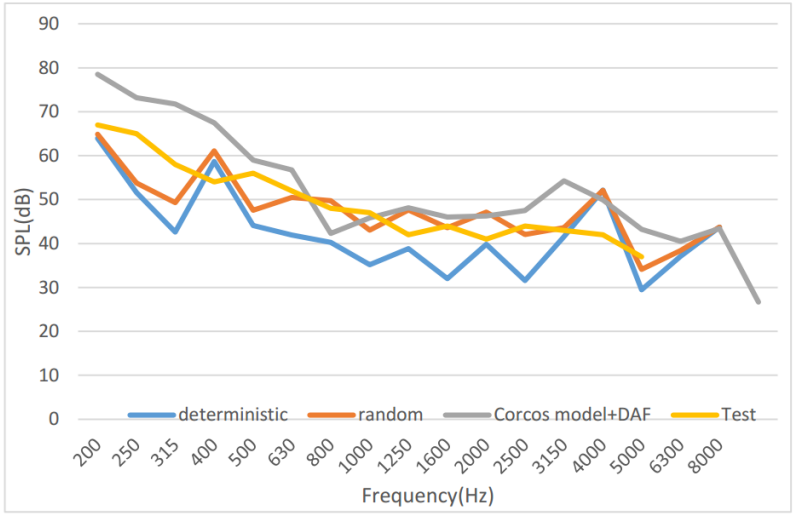

Fig. 13 – Radiated SPL comparison gained by different methods. (Deterministic:deterministic modal force coupled with BEM; Random:random modal force coupled with BEM; TBL+DAF: Corcos model coupled with BEM; Test, experimental results)

In order to compare how long each approach has taken to calculate radiated SPL of the panel, computing time of each step of different approaches is given in Table 3. The computing processes below are finished on a PC Workstation with Windows 7 64 bits, Intel(R) Xeon(R) 2×2.4GHz, 32GB RAM (No modeling time is included). Four procedures are included in each approach, which are reading CGNS files (result files of Fluent) and FFT, extracting convective component, extracting acoustic component and computing result. Extracting acoustic component procedure is not listed in Table 2, which cost about 40h by FM-BEM method.

In Table 3, we can see that there is nearly no difference of time for files reading and FFT between these three approaches. Corcos model coupled with BEM method saves much more time for the computing result procedure and costs also less time for extracting convective component. The other two approaches cost almost the same time.

Table 3 – Computing time of each approach

Approach	*Time of each procedure*			*Total time*
	Reading CGNS files and FFT	*Extracting convective component*	*Computing result*	
Corcos model coupled with BEM	*668.5s*	*Fitting Corcos parameters90.3s*	*0.34s*	*759.14s*
Deterministic modal force coupled with BEM	*667.01s*	*Modal analysis104.63s*	*252.97s*	*1024.61s*
Random modal force coupled with BEM	*660.13s*	*Modal analysis104.63*	*247.04s*	*1011.8s*

4. CONCLUSIONS

There are two different areas (separated area and reattached area) when flow passes the mirror, wavenumber-frequency method is used to analyze pressure PSD of these two regions, respectively. One can find that the convective speed in reattached area is faster and its direction is align with flow. However, convective speed in the separated region has two directions which means that vortex shed happens when flow passes the mirror. The magnitude of radiated sound is related not only to the excitation but also to the panel shape function. FSP of the panel based on CFD simulation in Fluent has been acquired to define as random or deterministic modal force load on the FE panel or as TBL load on a SEA panel. In order to extract the acoustic component, the FM-BEM is applied. Then three different methods are used to predict the radiated SPL at 0.1m far away from the panel. The results show that radiated SPL excited by convective component with acoustic component is 5-18dB higher than that without acoustic component within all three approaches at high frequency. Both these three approaches can be proved to be feasible and effective to calculate interior noise due to FSP from exterior flows. In addition, Corcos model coupled with BEM and random modal force coupled with BEM methods are better in terms of accuracy. Random modal force coupled with BEM method produces better result compared with experimental data. As for computing time, Corcos model coupled with BEM method costs less computing time obviously. These studied approaches can also be applied to full vehicle analysis. Based on accuracy and computing time, we can choose an appropriate approach in different design phases of a vehicle. More semi-empirical models (i.e. Chase, Efimstov, Goody etc.) used to compute the convective component are under the way.

5. ACKNOWLEDGEMENTS

The authors would like to thank the following project funding support. This report was prepared as an account of work sponsored by National Key R&D Program of China Number No.2017YFB0103204, Shanghai Science and Technology Innovation Action Plan No.18DZ1201703.

6. REFERENCES

1. P. G. Bremner, J. F. Wilby, “Aero-vibro-acoustics: problem statement and methods for simulation-based design solusion”, 8th AIAA/CEAS Aeroacoustics Conference & Exhibit, No. AIAA paper 2002-2551, 2002.
2. A. Hekmati, D. Ricot, P. Druault. “Vibroacoustic behavior of a plate excited by synthesized aeroacoustic pressure fields”, 16th AIAA/CEAS Aeroacoustics Conference, No. AIAA paper 2010-3950, 2010.
3. M. Smith, E.L. Iglesias, P.G. Bremner, etc. “Validation tests for flow induced excitation and noise radiation from a car window”, 18th AIAA/CEAS Aeroacoustics Conference, No. AIAA paper 2012-2201, 2012.
4. P. G. Bremner, “Vibroacoustic Source Mechanisms under Aeroacoustic Loads”, 18th AIAA/CEAS Aeroacoustics Conference, No. AIAA paper 2012-2206, 2012.
5. Mendonca, F., Shaw, T., Mueller, A. et al., “CFD-Based Wave-Number Analysis of Side-View Mirror Aeroacoustics towards Aero-Vibroacoustic Interior Noise Transmission,” SAE Technical Paper 2013-01-0640, 2013, doi: 10.4271/2013-01-0640.
6. Blanchet, D., Golota, A., Zerbib, N., and Mebarek, L., "Wind Noise Source Characterization and How It Can Be Used To Predict Vehicle Interior Noise," SAE Technical Paper 2014-01-2052, 2014, doi:10.4271/2014-01-2052.
7. R.Hold, A Brenneis, A Eberle, V. Schwarz & R. Siegert, “Numerical Simulation of Aeroacoustic Sound Generated by Generic Bodies Placed on a Plate, Part 1- Prediction of Aeroacoustic Sources”, Paper No. AIAA-99-1896, Proc. 5th AIAA/CEAS Aeroacoustic Conference, Bellevue WA, May 1999.
8. Y.P. WANG, Z.Q. GU, W.P. LI, et al., Evaluation of Aerodynamic Noise Generation by a Generic Side Mirror, World Academy of Science, Engineering and Technology 61 2010.
9. VA One 2015, The ESI Group. http://www.esi-group.com.